Surfactant Controlled Growth of Niobium Oxide Nanorods

Rana Faryad Ali,[†,‡] Amir H. Nazemi,[†,‡] Byron D. Gates[*,†]*

Final version published as Surfactant Controlled Growth of Niobium Oxide Nanorods, Ali, R.F.; Nazemi, A.; Gates, B.D., *Crystal Growth and Design*, 2017, 17 (9), 4637-4646.
https://doi.org/10.1021/acs.cgd.7b00500

[†] Rana Faryad Ali, Amir H. Nazemi, Prof. Byron D. Gates
Department of Chemistry and 4D LABS, Simon Fraser University, 8888 University Drive, Burnaby, BC, V5A 1S6, Canada

[*] E-mail: bgates@sfu.ca

[‡] These authors contributed equally to this work.

This work was supported in part by the Natural Sciences and Engineering Research Council (NSERC) of Canada (Grant No. 1077758), and through the Collaborative Health Research Projects (CHRP) Partnership Program supported in part by the Canadian Institutes of Health Research (Grant No. 134742) and the Natural Science Engineering Research Council of Canada (Grant No. CHRP 462260), the Canada Research Chairs Program (B.D. Gates, Grant No. 950-215846), and a Graduate Fellowship (Rana Faryad Ali) from Simon Fraser University. This work made use of 4D LABS (www.4dlabs.com) and the Center for Soft Materials shared facilities supported by the Canada Foundation for Innovation (CFI), British Columbia Knowledge Development Fund (BCKDF), Western Economic Diversification Canada, and Simon Fraser University.

Abstract

This paper describes a solution-phase hydrothermal synthesis of crystalline niobium pentoxide (Nb_2O_5) nanorods. The methods reported herein yield uniform Nb_2O_5 nanorods with average diameters of 6 nm and lengths of 38 nm, which are directly synthesized from niobic acid by a hydrothermal process. The formation of Nb_2O_5 nanorods from niobic acid was studied in the presence of surfactants that stabilize the nanostructures. The crystalline Nb_2O_5 nanorods were relatively uniform in size and shape. The size of the Nb_2O_5 nanorods could be tuned through the choice of surfactant even in the absence of a worm-like micellar morphology. Amine, amide, ammonium, carboxylate, sulfonate and sulfate containing surfactants were systematically evaluated for their influence on the ability to form uniform Nb_2O_5 nanorods. The surfactants in this study had hydrophobic tails that were either straight or branched, such as a polymer, and contained either a single or multiple head groups. The nanorods grew by a process of oriented attachment of nanoparticles that was regulated by the surfactants added into the reaction mixture. The results of these studies indicate that this synthetic approach serves as a tunable platform to prepare single crystalline niobium oxide based nanostructures with well-defined morphologies and dimensions. This surfactant assisted formation of crystalline Nb_2O_5 nanorods could also have important implications in the design of other transition metal oxide based nanomaterials.

Keywords: niobium pentoxide, Nb_2O_5, nanorods, crystalline, surfactant controlled growth

Introduction

We sought a versatile solution-phase method to prepare one-dimensional (1D) crystalline niobium pentoxide (Nb_2O_5) nanorods having a uniform size and shape. A controlled growth of Nb_2O_5 nanorods was evaluated using various surfactants while also examining the effect of these additives on the morphology and uniformity of the nanorods. Interest in 1D Nb_2O_5 based nanomaterials is in part for their relatively large surface area, anisotropic structure, and ease of doping with other metals.[1–3] These nanostructures have attracted attention for their potential use in a wide range of applications, such as support materials in catalysis,[4,5] electrochromic materials for display technologies,[6] cathodic materials in lithium ion batteries,[7] and substrates for gas sensing.[8] In addition, Nb_2O_5 is also an important raw material in the preparation of other metal niobates,[9] which themselves have properties of interest for piezoelectrics,[10] nonlinear optical materials,[11] photorefractive materials,[12] and photocatalytic substances.[13] Niobium oxide based nanomaterials are anticipated to continue to play an important role as both templates and components in the fabrication of electrochemical,[14] optoelectronic,[15] electromechanical,[16] and sensing devices.[17] Given this interest in nanoscale Nb_2O_5, several approaches have been developed recently for the preparation of these materials.

The techniques established to prepare nanomaterials of Nb_2O_5 are diverse. Common approaches to prepare 1D Nb_2O_5 nanomaterials include sol-gel methods, chemical vapor deposition (CVD), molten salt syntheses, electrospinning technologies and solvothermal methods.[18] Among these strategies, the sol-gel method using niobium alkoxides as precursors provides a simple wet chemical route to the synthesis of 1D Nb_2O_5 nanomaterials.[19] This approach does, however, have limitations that include the need for relatively expensive reagents, and for a high temperature treatment to induce crystallization of the product. Moreover, sol-gel preparation

of Nb_2O_5 nanomaterials also requires a well-controlled, and moisture free environment. The presence of moisture can have a significant influence on the hydrolysis of the precursor and, therefore, the morphology of the product.[20] A modified sol-gel method using electrophoretic driven templating has also been reported for the synthesis of Nb_2O_5 with better control over the morphology and uniformity of the product.[21] Morphology of Nb_2O_5 nanomaterials can also be controlled by CVD processes,[22] but these processes require relatively high reaction temperatures (400 ^oC to 600 ^oC), significantly longer processing times, and have a relatively low product yield.[23,24] Molten salt based syntheses can facilitate a rapid, large-scale growth of 1D Nb_2O_5 nanoscale materials through a relatively environmentally friendly approach.[25] It remains a challenge to extend control over the shape of the target products from the higher yielding syntheses using high temperature molten salts. The products prepared through molten salt based approaches also exhibit a significant degree of aggregation.[26,27] Electrospinning is an alternative approach to prepare 1D Nb_2O_5 nanomaterials of different lengths, and an ability to tune their diameter.[7] This method also requires high temperatures for calcination, but can produce fibers that have micrometer scale lengths.[28,29] Due to the number of disadvantages associated with prior methods, solution-phase methods have also been sought to prepare 1D Nb_2O_5 nanomaterials.

Solvothermal methods to prepare Nb_2O_5 nanomaterials have been recently reported with an improved control over size and shape of the products. A number of reaction parameters, such as reagent composition and concentration, and reaction temperature and duration can be adjusted through solvothermal methods to tune the size and shape of the products.[30,31] The solvothermal methods also provide control over the kinetics of the reaction, as well as crystal size, aggregation, and purity of the final products.[32] Zhang *et al.* prepared well-dispersed Nb_2O_5 nanorods using polyethylenimine as a template. The aspect ratio of these nanorods spanned from ~4.1 to ~22.4,

which were tuned by changing the pH of the reaction medium.[33] In another study, Luo *et al.* reported the synthesis of Nb_2O_5 nanorods having diameters of 50 nm and lengths up to several micrometers.[34] Wang and coworkers prepared arrays of Nb_2O_5 nanorods supported on a niobium foil through a hydrothermal process using H_2O_2 as the oxidant.[35] We have previously reported rod-like Nb_2O_5 nanostructures with an aspect ratio 3.4 ± 0.7 using a solution-phase non-hydrolytic method.[36] Disadvantages associated with these previously reported methods include relatively long reaction times (e.g., 2 to 30 days), an aggregated product, the need for subsequent heating of the products at high temperatures, and/or a requisite step to remove the template from the products.

Here, we introduce a surfactant mediated synthesis of Nb_2O_5 nanorods using a hydrothermal method. Advantages of this approach relative to prior art in preparing Nb_2O_5 nanorods include a shorter duration and lower temperature for the reaction and growth of the nanorods. This hydrothermal process starts with the synthesis of a precursor (niobic acid) using a modified method, which is followed by the growth of Nb_2O_5 nanorods in the presence of a surfactant. Growth of the Nb_2O_5 nanorods was evaluated in the presence of a series of different surfactants. These surfactants contained either amine, amide, ammonium, carboxylate, sulfonate or sulfate functional groups. We systematically examined the relative effects of these surfactants for their influence on the formation of niobium oxide nanorods. The phase evolution, morphology and crystallinity of Nb_2O_5 nanorods were characterized using X-ray powder diffraction (XRD), transmission electron microscopy (TEM), selected area electron diffraction (SAED), and high resolution transmission electron microscopy (HRTEM).

Experimental Section

Materials and Supplies

All the chemicals were of analytical grade and used as received without further purification. Niobium pentachloride ($NbCl_5$, 99.9%) and oleic acid (cis-9-octadecenoic acid, 90%) were purchased from Alfa Aesar. Sodium dodecyl sulfate (SDS, ≥98.5%), cetyltrimethylammonium bromide (CTAB, ≥96%), poly(allylamine hydrochloride) (PAH, 56k MW), polyvinylpyrrolidone (PVP, 1k MW), polyacrylic acid (PAA, 2k MW), trisodium 2-hydroxypropane-1,2,3-tricarboxylate (trisodium citrate, ≥99%), and cis-1-amino-9-octadecene (oleylamine, ≥98%) were obtained from Sigma Aldrich. Hydrogen peroxide (H_2O_2, 30% w/w aqueous solution), hydrochloric acid (HCl, 37% w/w aqueous solution) and 2-hydroxypropane-1,2,3-tricarboxylic acid (citric acid, 99.5%) were purchased from Caledon Laboratories, and poly(sodium 4-styrenesulfonate) (PSS, 70k MW) was provided by Scientific Polymers Products. Anhydrous ethanol and ammonium hydroxide (NH_4OH, 30% w/w aqueous solution) were purchased from Commercial Alcohols, and Fisher Scientific, respectively.

Synthesis of Niobic Acid

The niobium oxide precursor (i.e. niobic acid) was synthesized by modifying a previously reported method.[37] Briefly, 0.25 g of $NbCl_5$ was dissolved in 15 mL of ethanol, which results in the formation of a clear pale yellow solution. This step was followed by the formation of white precipitates through the addition of 3 mL of NH_4OH (28.0 to 30.0% NH_3 basis, w/w in water). The solution reached a pH of 9.6 following the addition of NH_4OH and precipitation of the white solids. These precipitates were isolated from solution by centrifugation at 13,500 rpm for 15 min. The isolated solid was washed three times with water to remove the NH_4Cl by-product, following each

rinse with another step of centrifugation at 13,500 rpm for 15 min. The purified niobic acid was obtained in the form of a white powder by drying the washed precipitates at 70 ^{o}C for 24 h.

Synthesis of Nb_2O_5 Nanorods

A hydrothermal method was used to prepare Nb_2O_5 nanorods. In a typical synthesis, 1 mM of surfactants was added to a 12 mL solution of hydrogen peroxide (30%, w/w in water) and stirred for 2 h. After this period of time, niobic acid (20.0 mg ± 1.0 mg) was added to the mixture and stirred for another 2 h at room temperature. The resulting suspension was added to a 23 mL Teflon lined autoclave (Model No. 4749, Parr Instruments Co., Moline, IL USA). The mixture was heated under autogenous pressure at 200 ^{o}C for 24 h followed by a slow cooling to room temperature. The white precipitates were washed three times with deionized water (18 MΩ·cm, produced using a Barnstead NANOpure DIamond water filtration system) using a process of centrifugation at 13,000 rpm for 15 min that involved decanting the supernatant, resuspension in deionized water and repeating this process. The purified and isolated product was dried at 80 ^{o}C for 24 h and the collected solids were characterized by a variety of analytical techniques.

Characterization of Nb_2O_5 Nanorods

Phase and crystallinity of the samples were determined from XRD patterns acquired with a Rigaku R-Axis Rapid diffractometer equipped with a 3 kW sealed tube copper source (Kα radiation, $\lambda = 0.15418$ nm) collimated to 0.5 mm. Powder samples were packed into a well (1 mm deep and 2 mm in diameter) drilled into a glass microscope slide (Leica 1 mm Surgipath Snowcoat X-tra Micro Slides). The particle morphology and size, and the crystallinity and lattice parameters of the Nb_2O_5 nanorods were each characterized using either an FEI Osiris X-FEG scanning/TEM operated at an accelerating voltage of 200 kV or a Hitachi 8000 TEM with a lanthanum hexaboride thermionic source operating at 200 kV. Samples were prepared for TEM analysis by dispersing an

isolated product in deionized water followed by drop casting 1 µL of this suspension onto a TEM grid (300 mesh copper grid coated with formvar/carbon) purchased from Cedarlane Labs. Each TEM grid was vacuum dried for at least 30 min prior to analysis.

Mean Lengths and Diameters of Nb_2O_5 Nanorods

The mean dimensions and their standard deviations for the nanorods were estimated by randomly selecting nanorods that were easily discernible from the other products as observed by TEM. The lengths and diameters of the nanorods were measured using the measurement tool in Adobe Acrobat Reader DC (version 6.0). The dimensions of at least 30 nanorods were measured using multiple TEM images to calculate the mean and standard deviation values for each sample. Histograms of the dimensions of the nanorods that were prepared either in the absence of SDS or the presence of 1 mM SDS, were created from measuring the dimensions of at least 55 nanorods from a series of TEM images. The standard deviation from the mean dimensions of each sample of Nb_2O_5 nanorods was calculated using Equation 1. The standard deviations reported here correspond to the first confidence interval or 1*s*.

Equation 1 $$s = \sqrt{\frac{1}{N-1}\sum_{i=1}^{N}(x_i - \overline{x})^2}$$

Here, s = standard deviation, $\overline{x}$ = the mean of all values, x_i = the individual values, and N = total number of values measured for one sample.

Results and Discussions

We sought to develop a simple hydrothermal method to prepare crystalline Nb_2O_5 nanorods and to control the growth of these nanorods through the addition of surfactants with specific polar functional groups. The morphology and aggregation of the resultant Nb_2O_5 nanorods were also examined through the relative effects of these additives.

Mechanism of the Formation of Nb_2O_5 Nanorods

Niobic acid was prepared by dissolving niobium pentachloride ($NbCl_5$) in ethanol, which led to a ligand exchange reaction between the chloride (Cl^-) and ethoxide ($C_2H_5O^-$) ligands for coordination with the niobium center (Nb^{5+}). The addition of NH_4OH (28.0 to 30.0% NH_3 basis, w/w in water) assisted in driving the ligand exchange reaction between Cl^- and $C_2H_5O^-$ to completion to form niobium ethoxide [$Nb(OEt)_5$].[38] A subsequent hydrolysis of the niobium ethoxide occurred due to the presence of water in the NH_4OH, which led to the formation of $Nb(OH)_5$ precipitates.[39] The soluble NH_4Cl by-product was removed by washing the solids with deionized water, and the purified and isolated precipitates were dried at 70 °C to obtain niobic acid ($Nb_2O_5 \cdot nH_2O$).

The growth of Nb_2O_5 nanorods from niobic acid under hydrothermal treatment was pursued through a process of dissolution and crystallization. Niobic acid was peptized in an aqueous solution of H_2O_2 (30%, w/w) containing amine, amide, ammonium, carboxylate, sulfonate or sulfate functionalized surfactants to control the growth of the Nb_2O_5 nanorods. This peptization process initiates cleavage of the oxo and hydroxo bridges in niobic acid due to the high reactivity of niobium ions (i.e. Nb^{5+}) with H_2O_2. The introduction of H_2O_2 results in the formation of peroxo ions, O_2^{2-}, in solution, which will coordinate with Nb^{5+}. The resulting mixture leads to the formation of a sol of niobic acid. During the hydrothermal treatment, the sol could dehydrate at the elevated processing temperatures and oxidizing conditions of the reaction. This process likely forms monomers of Nb_2O_5. The reaction mixture would be supersaturated with monomers that initiated the nucleation of Nb_2O_5 seeds. The growth of anisotropic Nb_2O_5 nanorods from these monomers and seeds likely occurs through a process of oriented attachment of the Nb_2O_5 nanocrystals (Figure 1a).[40] This oriented attachment is likely driven by a permanent dipole

moment within the nanocrystals due to an anisotropic distribution of surface charges. This dipole arises from differences in the atomic distribution of Nb and O on the surfaces of the nanocrystals and differences in the electronegativities of these elements. A relatively large dipole moment is predicted to form along the [001] direction.[41,42] Smaller dipoles formed along the other crystal directions were anticipated to have less influence on the self-organization of the nanoparticles. The adsorption of surfactant molecules onto the surfaces of the nanocrystals may have also significantly decreased the surface energies of some facets in comparison to the {001} facets. These combined effects lead to a relatively large dipole moment along the [001] direction, which resulted in dipole interactions between individual nanoparticles and the oriented attachment of these nanocrystals along the [001] direction. The result was a subsequent formation of 1D nanostructures *vide infra*.[43] A TEM analysis of the products confirmed the formation of 1D Nb_2O_5 nanorods from the hydrothermal treatment of the niobic acid in the presence of surfactants (Figures 1b, 1c). Some surfactants can form worm-like micelles that could be used to promote the growth of 1D nanostructures by directing the assembly of the seeds and monomers during growth.[44] The formation of Nb_2O_5 nanorods was, however, achieved in the absence of worm-like micellar templates. This observation further supports the proposed anisotropic growth of the Nb_2O_5 nanorods due to an oriented attachment of nanocrystals.

The Role of Surfactants in the Solution-Phase Synthesis and Colloidal Stability of Nb_2O_5 Nanorods

Solution-phase methods utilizing surfactants have been used to prepare a variety of nanostructures including anisotropic nanomaterials.[45] Surfactants are typically chosen for their amphiphilic characteristics (i.e. having a polar head group and a non-polar tail). The head groups are primarily hydrophilic in nature and often contain hetero-atomic functional groups (e.g., amines, sulfates, carboxylates), while their tails are usually composed of hydrocarbon chains.[46] The polar

and non-polar components of this type of surfactant can each play important roles in the surfactant mediated synthesis of nanomaterials. The hydrophobic chains can interact with the surfaces of the nanoparticles to form compact monolayers or bilayers due to the van der Waals interactions between neighboring chains. The polar head groups can present charges on the surfaces of nanostructures that minimize aggregation of the nanoparticles due to the repulsive charges on their surfaces. A strong adsorption of ionic surfactants onto the surfaces of nanocrystals can also minimize the exchange of surfactant molecules, which can be used to control the growth of these nanostructures.[47,48] The resultant control over growth of the nanostructures can also be utilized to direct the formation of some rod-like nanostructures.[49,50] Amine, amide, ammonium, carboxylate, sulfonate or sulfate containing surfactants were screened for their relative influence on the formation of Nb_2O_5 nanorods.

Surfactant molecules adsorbed onto the surfaces of the nanorods can also determine the colloidal stability of the particles and the strength of their interactions. We evaluated the ease of dispersing each of the surfactant stabilized Nb_2O_5 nanorods into aqueous media. The nanorods remained well-dispersed in solution for at least 24 h. This colloidal stability of the nanorods was attributed to the polar, water soluble surfactant molecules evaluated in this study. After 1 day, the nanorods began to settle from solution. More than half of the nanorods had settled from these aqueous suspensions after a period of 2 days. Colloidally stable Nb_2O_5 nanorods were synthesized using each of the surfactants. The quality of each of these products did, however, vary in terms of their size distribution and yield, as measured by TEM. We performed a systemic investigation to identify an optimal type of surfactant for preparing Nb_2O_5 nanorods that are uniform in size and shape, and that exhibit colloidal stability.

Growth of Nb_2O_5 Nanorods in the Presence of Amine, Amide, or Ammonium Containing Surfactants

We explored the use of four different nitrogen containing surfactants to control the growth of the Nb_2O_5 nanorods. These surfactants included oleylamine (OAm) and poly(allylamine hydrochloride) (PAH) containing a primary amine ($–NH_2$), as well as cetyltrimethylammonium bromide (CTAB), and polyvinylpyrrolidone (PVP) containing a quaternary ammonium and an amide, respectively. Both PVP and PAH have branched hydrophobic backbones, while CTAB and OAm each contain a linear hydrocarbon tail. Each of these surfactants have been previously used to prepare a variety of nanomaterials, such as metal oxides (e.g., Fe_3O_4, Mn_3O_4, CoO, Fe/Fe_3O_4, ZnO),[51] plasmonic nanostructures (e.g., Ag, Au, Cu),[52,53] electrocatalytic nanomaterials (e.g., Pt and Pd based nanostructures),[54,55] semiconductor nanomaterials (e.g., CdSe, PbTe, CuS)[56] and hetero-structural nanomaterials [e.g., $NaLa(MoO_4)_2$].[57,58] These nitrogen containing surfactants can play an important role in regulating the growth and mitigating aggregation of the nanomaterials, but these properties depend on the specific interactions between the surfactants and the nanocrystals.

We studied the relative effects of a series of nitrogen containing surfactants on the growth of Nb_2O_5 nanorods. Each surfactant was evaluated at a concentration of 1 mM as determined from the moles of the nitrogen containing functional groups in solution. The concentration of niobic acid, volume of solvent, duration of the reaction, and reaction temperature remained unchanged between each of these syntheses. The mean lengths and diameters of the nanorods (Table 1) were determined from analysis of the TEM data (Figure 2). Relatively well-dispersed and uniform nanorods were obtained from the addition of OAm (Figure 2a) in contrast to the CTAB capped nanorods (Figure 2b). The average length of nanorods prepared in the presence of CTAB were

smaller (excluding the larger aggregates) than the OAm capped nanorods. The formation of a more aggregated and less uniform product in the presence of CTAB might be due to its cationic polar head group, which could cause charge neutralization at the surfaces of the nanocrystals.[59] Grzelczak *et al.* also observed that the relatively poor solubility of CTAB in aqueous solvents can promote the aggregation of nanomaterials.[60] This charge neutralization and/or poor solubility could decrease the stability of both the nanoparticles and the resulting nanorods.

The nitrogen functionalized polymers hindered the formation of the nanorods. The presence of PVP or PAH yielded a relatively poor product (Figures 2c, 2d). The amide functionality and the large structure of the pyrrolidone moiety within PVP might introduce inter-chain dipoles and steric hindrance. The result could be a weaker interaction of the surfactant molecules with the Nb_2O_5, leading to the formation of a non-uniform, aggregated product.[61] Yields of the nanorods prepared in the presence of OAm, PAH and CTAB were higher than those prepared through the use of PVP as determined from the TEM analyses (Table 1). The average lengths and diameters of nanorods prepared in the presence of PAH and PVP (excluding the larger aggregates) were smaller than those prepared through OAm or CTAB mediated growth. The smaller dimensions of the PAH or PVP capped nanorods might be due to the extended structures of these polymers, which could decrease the interactions between some of the nanoparticles. The variability of these interactions does, however, lead to the formation of a less uniform product.

The presence of cationic surfactants (e.g., CTAB, PAH) yielded nanorods with a relatively high degree of aggregation. To further evaluate the influence of charged surfactants on the formation of the Nb_2O_5 nanorods, the pH of the solution containing OAm was decreased to form an ammonium ion head group ($R\text{-}NH_3^+$). Aspect ratio of the resulting nanorods decreased and the synthesis yielded a range of other shapes (e.g., squares and spheres) as observed by TEM (Figure

S1). This poorer control over the growth of the Nb_2O_5 nanostructures is attributed to screening of their dipole induced interactions, which inhibited the process of oriented attachment. The interactions of other charged surfactants will be explored in further detail below.

The crystallinity of the nanorods stabilized with nitrogen containing surfactants was confirmed by XRD analysis. Powder XRD patterns were acquired for each of these products (Figure 2). It is, however, known that CTAB itself can form crystalline rod-like nanostructures.[62,63] It was important to confirm the presence of crystalline nanorods of Nb_2O_5. Rod-like nanostructures were observed in the TEM analysis of a mixture of niobic acid and CTAB before processing this mixture in the autoclave (Figure S2). This mixture of niobic acid and CTAB was analyzed by XRD before hydrothermal treatment, as well as after processing in an autoclave (Figure S3). Two broad peaks in the XRD pattern obtained before hydrothermal treatment corresponded to XRD patterns reported for niobic acid.[64] This diffraction pattern indicated the amorphous nature of the sample, and suggested the rod-like structures observed by TEM might be assemblies of CTAB forming worm-like micellar structures. After hydrothermal treatment, relatively sharp and well-defined diffraction peaks appeared in the XRD pattern confirming the formation of a crystalline product. The diffraction patterns was indexed to crystalline Nb_2O_5, further indicating that hydrothermal treatment was necessary to form the Nb_2O_5 nanorods. The XRD patterns of each of the samples of Nb_2O_5 nanorods prepared in the presence of nitrogen containing surfactants matched those of the pseudo-hexagonal structure of Nb_2O_5 (space group: P6/mmm. JCPDS No. 28-0317). The relative intensities of the diffraction peaks observed for the nanorods were different from the intensities observed in the standard patterns for the bulk reference material. These differences were attributed to the preferred growth of the nanorods along specific directions within the crystalline product. A relatively intense and narrow peak at a 2-theta value of 22.8° for all of the products corresponded

to diffraction from the {001} facets of Nb_2O_5. The more intense diffraction peak associated with reflections from the (001) planes in contrast to those from the (100) planes supported the observation that the nanorods tended to grow along the [001] direction.

The average dimensions of the crystallites in the products stabilized with nitrogen containing surfactants were calculated using the Scherrer equation.[65] The diffraction assigned to the (001) planes of Nb_2O_5 were significantly sharper than the other peaks. A comparative analysis was applied to the peaks corresponding to the [001] and [100] growth directions, which are mutually perpendicular to each other. The corresponding diffraction peaks were centered at 2-theta values of 22.8° and 28.0°, respectively. The average calculated dimensions of the crystallites were between ~7 nm and ~12 nm for the [001] growth direction. There was, however, a large variation between these dimensions and those measured by TEM (Table 1). The inaccuracy of particle size determination by analysis of the XRD data is likely due to the non-spherical crystallites. Anisotropic nanomaterials are not accurately described when assuming a symmetric peak shape for individual values of 2-theta.[66,67] The assessment by TEM ignored the dimensions of the larger structures observed in the products, but this analysis more accurately assessed the influence of each of the nitrogen containing surfactants on the uniformity and yield of the nanorods.

Growth of Nb_2O_5 Nanorods in the Presence of Carboxylate, Sulfonate and Sulfate Containing Surfactants

We also investigated the formation of Nb_2O_5 nanorods using a series of carboxylate, sulfonate or sulfate containing surfactants. The surfactants chosen for this study have also been widely used in the synthesis of nanomaterials.[68,69] For example, oleic acid (OA) is commonly used to prepare magnetic nanoparticles, such as through hydrothermal methods, co-precipitation methods, or the thermal decomposition of organometallic precursors.[70,71] This surfactant is also used as co-

surfactant in the synthesis of nanostructures of noble metals (e.g., Au, Ag) and transition metal oxides (e.g., Nb_2O_5, TiO_2).[72,73] A complementary surfactant to OA is polyacrylic acid (PAA), which is a water-soluble anionic polymer that has been used to prepare nanoparticles of metal oxides, such as $CoFe_2O_4$.[74] This polymer is also an important sub-unit in block copolymers (e.g., PS-b-PAA, PMMA-b-PAA) used in the synthesis of Au-based nanostructures.[75] Citric acid and sodium citrate are also commonly used carboxylate containing surfactants in the synthesis of noble metals (e.g., Au, Ag), and magnetic iron oxide based nanoparticles.[69] These citrate based surfactant molecules can coordinate to the surfaces of the particles through the carboxylate groups. These citrate capped nanoparticles are typically well-dispersed due to electrostatic stabilization through the uncoordinated carboxylate groups, but these capping groups are also easily displaced from the surfaces of the nanoparticles.[76,77] For evaluating surfactants containing a sulfate or sulfonate group, Nb_2O_5 nanorods were grown in the presence of sodium dodecyl sulfate (SDS) or polystyrene sulfonate (PSS). The SDS have a hydrocarbon tail with a single hydrophilic sulfate head group in contrast to the PSS that contain a polymeric backbone with a repeating negatively charged benzenesulfonic sub-unit. Both SDS and PSS are commonly used as surfactants for the preparation of oxide containing nanoparticles (e.g., Fe_3O_4, $CoFe_2O_4$, SiO_2) and nanostructures of noble metals (e.g., Au, Ag, Pd).[78–80] Many other carboxylic, sulfonic or sulfate containing surfactants are also used in the preparation of nanostructures, but a subset is pursued here as a comparative study to identify general trends in controlling the growth of Nb_2O_5 nanorods. The aim is to identify a type of surfactant that can control the growth and prevent aggregation of the nanomaterials.

A series of carboxylic acid functionalized surfactants were compared for their effectiveness in controlling the preparation of Nb_2O_5 nanorods. The TEM images and XRD analyses of these Nb_2O_5 nanorods are shown in Figure 3. Relatively well-dispersed and uniform nanorods were

formed in the presence of OA in comparison to the other three carboxylate containing surfactants. For OA and PAA based syntheses, the average diameters and lengths of the resulting nanorods were nearly identical (Table 2). For the citric acid (Figure 3c) and trisodium citrate (Figure 3d) mediated syntheses, the products were relatively aggregated and non-uniform in comparison to the nanorods prepared through the OA or PAA assisted growth. The highest degree of aggregation was observed for the products prepared in the presence of the trisodium citrate. The more evenly dispersed nanorods capped with OA or PAA could be due to a larger contribution from the van der Waals forces within these capping layers and with the surfaces of the nanocrystals. These interactions effectively controlled the oriented attachment and growth of the nanocrystals. The OA and PAA surfactants produced a highly anisotropic product while also minimizing aggregation of the nanorods. The more evenly dispersed products capped with OA might be due to its relatively long hydrocarbon tail and single carboxylate head group, which exhibit the ability to assemble into monolayers or bilayers on the surfaces of the nanocrystals.[81,82] For PAA, the multiple –COOH groups along its hydrocarbon backbone and the steric hindrance between separate polymer chains may decrease its effectiveness to passivate the surfaces of the nanocrystals.[83] A lower surface packing density of PAA relative to OA could lead to the decreased yield and increased aggregation of the PAA stabilized product. The citrate based surfactants have even weaker forces of interaction with the surfaces of the nanorods.[84] These weaker interactions are likely responsible for the less uniform dimensions and higher degree of aggregation observed for these nanorods. In summary, surfactants with relatively strong and regular interactions with the surfaces of nanocrystals yield more uniform and stable Nb_2O_5 nanorods.

The preparation of niobium oxide nanorods was extended to surfactant systems containing a sulfate or sulfonate to further evaluate the influence of the functional groups on the yield and

uniformity of the product. The SDS capped nanorods were more uniformly dispersed than the PSS mediated synthesis, but each of these synthetic routes produced a relatively uniform product (Figure 4). The average diameters and lengths of the Nb_2O_5 nanorods prepared in the presence of SDS were smaller than those prepared through the PSS mediated growth (Table 2). In the SDS mediated growth, the uniform dispersion and smaller size of the nanorods could be attributed to the single polar head group, and the ability of this molecule to assemble into more tightly packed monolayers or bilayers on the surfaces of the nanocrystals.[85] The larger head group of the aryl sulfonate on the PSS and the flexibility of the polymer chain could lead to lower quality coatings on the nanocrystals, but the π-stacking and van der Waals interactions of the aryl groups could balance these qualities. The properties of the PSS are sufficient to passivate the nanorods during their growth as observed in the regularity of the product, but could also lead to the observed particle aggregation.[86] Interestingly, the yield of nanorods was relatively higher for most of the carboxylic, sulfonic and sulfuric acid containing surfactants than those products prepared in the presence of amine, amide or ammonium containing surfactants.

The crystallinity of the nanorods prepared in the presence of carboxylate, sulfonates or sulfate containing surfactants was investigated through powder XRD analyses. The observed XRD diffraction peaks were similar (Figures 3 and 4) to those observed for Nb_2O_5 nanorods prepared with nitrogen containing surfactants (Figure 2) and were indexed to the pseudo-hexagonal structure of Nb_2O_5 (space group: P6/mmm. JCPDS No. 28-0317). The relatively intense peaks at a 2-theta value of 22.8^o further indicated a dominant growth of the nanorods along the [001] direction. The average dimensions of the crystallites in the nanorods were calculated based on the diffraction peaks at 22.8^o and 28.0^o using the Scherrer equation (Table 2). A large variation was observed between the dimensions of the nanocrystallites calculated using the diffraction from the

(001) planes in contrast to lengths of the nanorods as measured by TEM. Dimensions of the nanocrystallites calculated using the diffraction from the (100) planes were, however, comparable to the widths of the nanorods prepared in the presence of SDS. As mentioned above, the large variation in the dimensions of the nanorods as determined from TEM and XRD measurements is attributed to the anisotropic growth of the nanorods. The XRD analyses did confirm the successful preparation of crystalline Nb_2O_5 regardless of the type of surfactant used in the synthesis of the nanorods.

The crystallinity of the anisotropic Nb_2O_5 nanostructures was further analyzed using high resolution transmission electron microscopy (HRTEM) and selected area electron diffraction (SAED). The HRTEM analyses of the nanorods prepared from the PSS and SDS mediated syntheses are shown in Figures 4c and 4d, respectively. The observed lattice fringe patterns suggest that the as-synthesized products were single crystalline nanorods. The separation of adjacent lattice fringes (or d-spacing) was 3.9 Å ± 0.3 Å, which matches with the inter-planar spacing of the (001) crystal planes. To compliment this analysis, SAED patterns were acquired using a large area aperture to simultaneously analyze multiple Nb_2O_5 nanorods (Figure S4). The ring patterns from the SAED revealed a dominated diffraction along the [001] direction in agreement with the XRD and HRTEM analyses. These results further confirmed growth of the nanorods along the [001] direction. The composition of the Nb_2O_5 nanorods were further evaluated using Raman spectroscopy techniques (Figures S5 and S6). The presence of a series of Raman peaks between 1000 cm^{-1} and 100 cm^{-1} confirmed the formation of pseudo-hexagonal Nb_2O_5 in agreement with previous reports.[87] The distinct Raman scattering patterns in the region between 1800 cm^{-1} and 1000 cm^{-1} further confirmed the presence the different surfactants on the surfaces of the Nb_2O_5 nanorods (Figures S5 and S6).

Effect of Surfactant Concentration on the Growth of Nb_2O_5 Nanorods

To further understand the influence of surfactants on growth of the Nb_2O_5 nanorods, we systematically investigated the effect of changing the concentration of surfactants in solution. Holding all other variables constant, Nb_2O_5 nanorods were prepared in the presence of varying amounts of SDS. The critical micelle concentration (CMC) of SDS is 8.2 mM.[82] The growth of nanorods was explored at SDS concentrations both above and below its CMC (Figure 5). Nanoparticles, but not highly anisotropic nanostructures, were observed at 100 mM SDS and the product exhibited a high degree of agglomeration (Figure 5a). Decreasing the SDS concentration to 10 mM led to the formation of distinct nanorods (Figure 5b). A thin layer of surfactant persisted on the surfaces of the products prepared at either 100 mM or 10 mM SDS, even after carefully washing the products. A further decrease in the concentration of SDS to 1 mM and 0.1 mM resulted in the formation of relatively well-dispersed and nearly uniform nanorods (Figures 5c, 5d). The nanorods prepared using 10 mM SDS were larger than those prepared at lower concentrations (1 mM and 0.1 mM) of SDS. By decreasing the concentration of SDS to 0.01 mM the hydrothermal process still yielded nanorods, but these products also agglomerated into larger rod-like structures (Figure 5e). These results demonstrated that the nanorods growth was not the result of the formation of micellar-like assemblies of the surfactants since nanorods still formed at concentrations below the CMC of SDS. A control experiment was also performed in the absence of any surfactants added to the reactants. This growth of nanorods in the absence of SDS further evaluated the influence of the added surfactants on the morphology and aggregation of the product (Figure 5f). These nanorods had nearly the same aspect ratio as those prepared in the presence of 0.01 mM SDS. The product synthesized without SDS was, however, more agglomerated and had a higher yield of relatively large rod-like structures than those prepared with 0.01 mM SDS (Figure

S7). Crystallinity of each of these products was characterized by XRD analysis. All peaks in the XRD diffraction patterns were similar to those for the other syntheses of Nb_2O_5 nanorods (Figure S8). The intensity of the diffraction from the (001) planes initially increased and then decreased with an increase in concentration of SDS from 0.1 mM to 100 mM. Low concentrations of SDS are insufficient to stabilize the process of oriented attachment needed for a high yield of nanorods. High concentrations of SDS likely hinder growth of the nanorods along the [001] direction, leading to a non-uniform, agglomerated product. An optimal concentration of surfactant was necessary to assist in the process of oriented attachment and the formation of a dispersed product of uniform nanorods. Nanorods prepared in the absence of SDS had larger aspect ratio than those prepared in the presence of SDS, even if the contributions of aggregates and agglomerates are ignored (Figure S7). For example, in the presence of 1 mM SDS the Nb_2O_5 nanorods had a diameter of 5 ± 1 nm and length of 25 ± 4 nm in contrast to a nominal diameter of 5 ± 1 nm and length of 33 ± 12 nm for nanorods synthesized without any surfactant (Figure S9). Aspect ratio of the nanorods prepared in the presence of the SDS (i.e. 5.0) was smaller than that achieved for nanorods synthesized in the absence of surfactants (i.e. 6.6). The nanorods prepared in the presence of 1 mM SDS were shorter, but had a more uniform size distribution. These results indicated that the growth of the nanorods by oriented attachment and aging was effectively controlled by the surfactants. Surfactants play an important role in regulating the growth of the Nb_2O_5 nanocrystals. It may be possible to further improve the uniformity of the product by identifying a more suitable surfactant. The lessons from this systemic investigation into the surfactant mediated synthesis of Nb_2O_5 nanorods could also be adapted to controlling the formation and dispersion of other metal oxides nanostructures.

Conclusions

In summary, we successfully prepared a series of crystalline Nb_2O_5 nanorods by investigating the relative effects of amine, amide, ammonium, carboxylate, sulfonate or sulfate containing surfactants on the growth of these nanorods. Well-dispersed and uniform nanorods were successfully prepared using a surfactant assisted hydrothermal method. Crystalline Nb_2O_5 nanorods were obtained without requiring further thermal processing. These products exhibited growth predominantly along the [001] direction of the pseudo-hexagonal phase of Nb_2O_5. The single crystalline and anisotropic nature of the Nb_2O_5 nanorods is the result of the surfactant mediated oriented attachment of nanocrystals. The surfactants used in these syntheses improved the dispersion of the nanorods and assisted in achieving nanorods of relatively small dimensions. Many of the surfactants effectively interacted with the surfaces of the nanocrystals, which regulated the growth of the nanorods. The surfactants used to assist the growth of the nanorods had either polymeric or linear hydrocarbon tails containing either multiple or single polar functional groups, respectively. Due to the amphiphilic nature of these surfactants, the polar functional groups extending from the surfaces of the nanorods minimized the aggregation of individual nanorods. Syntheses mediated by carboxylate, sulfonate and sulfate containing surfactants yielded more nanorods than syntheses assisted by the addition of amine, amide or ammonium functionalized surfactants. This surfactant controlled growth of the Nb_2O_5 nanorods could be extended to the preparation of nanostructures of other transition metal oxides with the aim of controlling the product uniformity and their dispersion if synthesized through a similar mechanism of oriented attachment.

Tables

Table 1. Average dimensions of Nb_2O_5 nanorods stabilized with amine, amide or ammonium containing surfactants.

surfactant*	mean length (nm)†	mean diameter (nm)†	average crystallite sizes (nm)		approximate yield of nanorods (%)
			[001]‡	[100]‡	
OAm	72 ± 14	6 ± 2	11.9	2.8	75
CTAB	46 ± 9	9 ± 1	7.1	17.3	50
PVP	20 ± 2	6 ± 1	8.8	5.4	20
PAH	28 ± 5	5 ± 1	6.9	2.9	65

* Abbreviations: OAm = oleylamine; CTAB = cetyltrimethylammonium bromide; PVP = polyvinylpyrrolidone; and PAH = poly(allylamine hydrochloride).
† Dimensions of the nanorods determined by TEM analysis.
‡ Dimensions of the crystallites calculated using the Scherrer equation.

Table 2. Average dimensions of Nb_2O_5 nanorods capped with carboxylate, sulfonate, or sulfate containing surfactants.

surfactant*	mean length (nm)†	mean diameter (nm)†	average crystallite sizes (nm)		approximate yield of nanorods (%)
			[001]‡	[100]‡	
PAA	34 ± 3	5 ± 1	11.2	2.6	85
OA	36 ± 5	5 ± 1	9.2	2.7	90
citric acid	40 ± 4	9 ± 2	8.4	2.8	60
trisodium citrate#	-	-	10.3	2.6	5
PSS	38 ± 4	6 ± 1	11.5	2.9	80
SDS	25 ± 4	5 ± 1	11.3	4.6	83

* Abbreviations: OA = oleic acid; PAA = polyacrylic acid; PSS = poly(sodium 4-styrenesulfonate); and SDS = sodium dodecyl sulfate.
# The product prepared in the presence of trisodium citrate was highly aggregated, which made it difficult to accurately analyze the dimensions of the nanorods.
† Dimensions of the nanorods determined by TEM analysis.
‡ Dimensions of the crystallites calculated using the Scherrer equation.

Figures and Captions

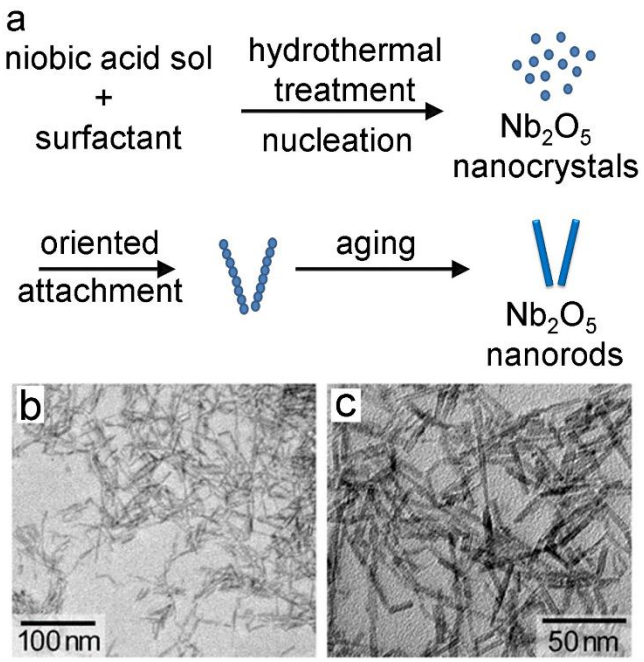

Figure 1. (a) A proposed mechanism for the synthesis of anisotropic Nb_2O_5 nanorods prepared from a niobic acid sol. During hydrothermal treatment, crystalline seeds nucleate and grow in the presence of the niobic acid sol and added surfactants. The surfactant capped nanocrystals undergo a process of oriented attachment and an aging process that results in the formation of anisotropic Nb_2O_5 nanorods. (b,c) Representative transmission electron microscopy (TEM) images of the resultant Nb_2O_5 nanorods.

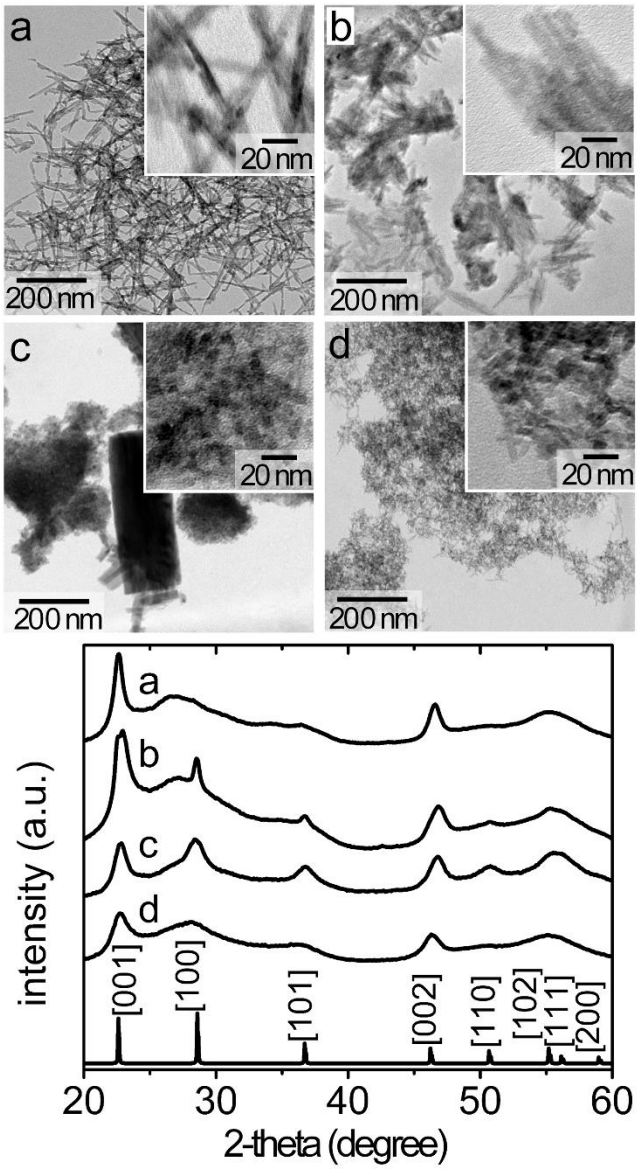

Figure 2. Transmission electron microscopy (TEM) images and X-ray powder diffraction (XRD) patterns of niobium pentoxide nanorods synthesized at 200 ^{o}C from niobic acid in the presence of: (a) *cis*-1-amino-9-octadecene or oleylamine; (b) cetyltrimethylammonium bromide or CTAB; (c) polyvinylpyrrolidone or PVP; and (d) poly(allylamine hydrochloride) or PAH. Concentrations were adjusted to maintain 1 mM of surfactant molecules in solution (concentrations were set to 1 mM of individual subunits for the polymers). A reference XRD pattern is included with indexing for pseudo-hexagonal Nb_2O_5 (JCPDS No. 28-0317).

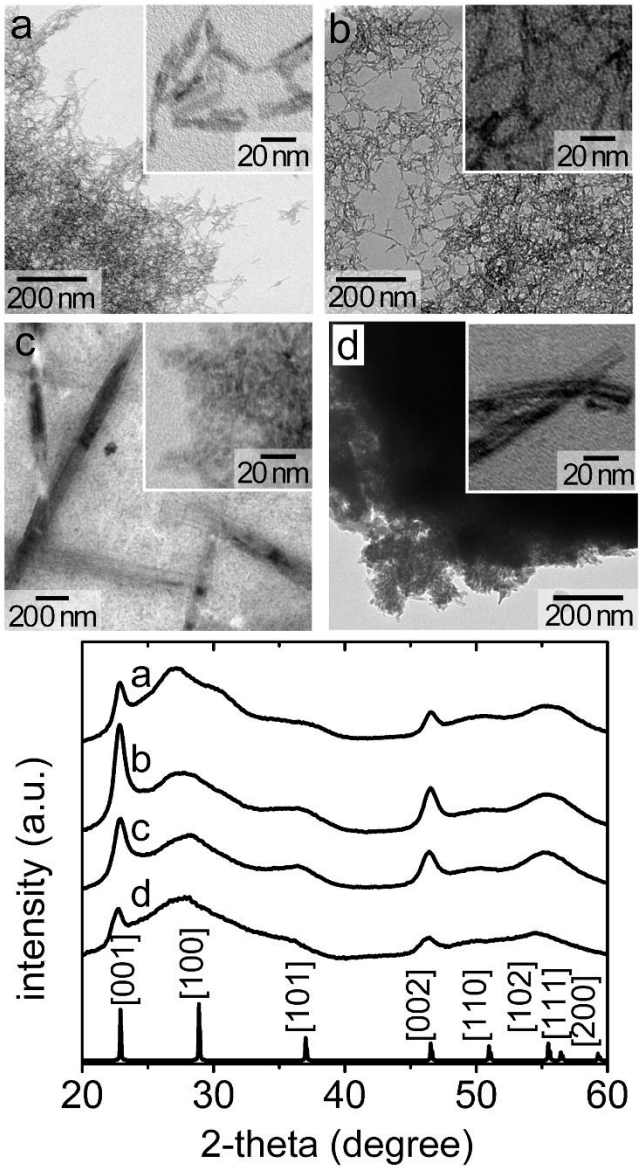

Figure 3. Niobium oxide nanorods, as imaged by TEM, and analyzed by XRD following their synthesis in the presence of: (a) poly(acrylic acid) or PAA; (b) *cis*-9-octadecanoic acid or oleic acid; (c) citric acid; and (d) trisodium citrate. Each of these syntheses was carried out at 200 ^{o}C in an autoclave. Surfactant concentrations were adjusted to maintain 1 mM of the surfactant molecules in solution (concentrations were set to 1 mM of individual subunits of the polymer). A fully indexed reference XRD pattern is also included for pseudo-hexagonal Nb_2O_5 (JCPDS No. 28-0317).

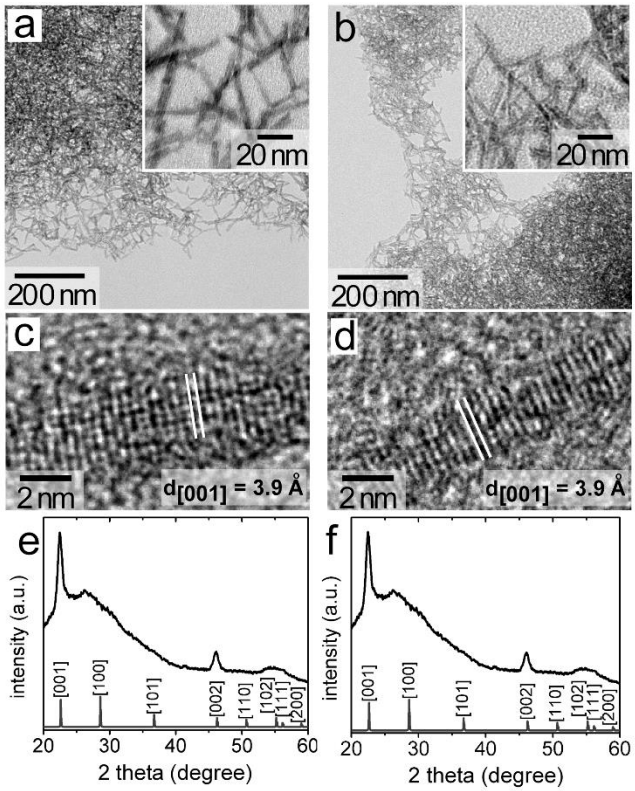

Figure 4. Transmission electron microscopy images of niobium pentoxide nanorods synthesized from niobic acid in the presence of: (a, c) poly(4-styrenesulfonic acid) sodium salt (PSS); and (b, d) sodium dodecyl sulfate (SDS). X-ray powder diffraction patterns confirm a pseudo-hexagonal Nb_2O_5 product with a dominant growth orientation of [001] when synthesized with (e) PSS or (f) SDS. Reference XRD patterns are included for pseudo-hexagonal Nb_2O_5 (JCPDS No. 28-0317).

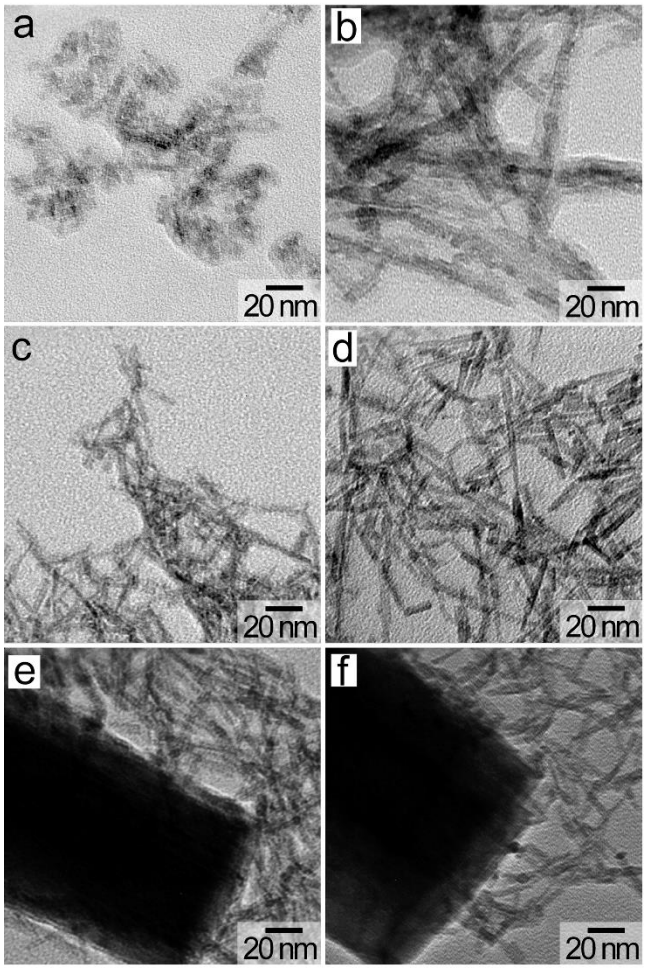

Figure 5. Niobium oxide nanoparticles, imaged by TEM, after their synthesis in the presence of decreasing concentrations of SDS: (a) 100 mM SDS; (b) 10 mM SDS; (c) 1 mM SDS; (d) 0.1 mM SDS; (e) 0.01 mM SDS; and (f) without the addition of surfactant.

References

(1) Liu, J.; Xue, D.; Li, K. *Nanoscale Res. Lett.* **2011**, *6* (1), 1–8.
(2) Hu, Y.; Gu, H.; Wang, Z. *The Anisotropic Growth of Perovskite Oxide Nanowires*; In Nanowires - Fundamental Research; INTECH: Rijeka, Crotia, **2011**, 141–160.
(3) Zhou, Y.; Li, G.; Zeng, J.; Zheng, L.; Zhao, K.; Ruan, W. *Ceram. Int.* **2015**, *41*, S152–S156.
(4) Prado, A. G. S.; Bolzon, L. B.; Pedroso, C. P.; Moura, A. O.; Costa, L. L. *Appl. Catal. B Environ.* **2008**, *82* (3), 219–224.
(5) Carniti, P.; Gervasini, A.; Marzo, M. *J. Phys. Chem. C* **2008**, *112* (36), 14064–14074.
(6) Mozetič, M.; Cvelbar, U.; Sunkara, M. K.; Vaddiraju, S. *Adv. Mater.* **2005**, *17* (17), 2138–2142.
(7) Viet, A. Le; Reddy, M. V; Jose, R.; Chowdari, B. V. R.; Ramakrishna, S. *J. Phys. Chem. C* **2009**, *114* (1), 664–671.
(8) Wang, Z.; Hu, Y.; Wang, W.; Zhang, X.; Wang, B.; Tian, H.; Wang, Y.; Guan, J.; Gu, H. *Int. J. Hydrogen Energy* **2012**, *37* (5), 4526–4532.
(9) Hsiao, Y.-J.; Chang, Y.-H.; Chang, Y.-S.; Fang, T.-H.; Chai, Y.-L.; Chen, G.-J.; Huang, T.-W. *Mater. Sci. Eng. B* **2007**, *136* (2), 129–133.
(10) Wu, J. *RSC Adv.* **2014**, *4* (96), 53490–53497.
(11) Dutto, F.; Raillon, C.; Schenk, K.; Radenovic, A. *Nano Lett.* **2011**, *11* (6), 2517–2521.
(12) Sidorov, N. V; Yanichev, A. A.; Gabain, A. A.; Palatnikov, M. N.; Smirnov, A. N. *J. Appl. Spectrosc.* **2013**, *80* (2), 226–231.
(13) Wang, L.; Wang, W.; Shang, M.; Sun, S.; Yin, W.; Ren, J.; Zhou, J. *J. Mater. Chem.* **2010**, *20* (38), 8405–8410.
(14) Yan, L.; Rui, X.; Chen, G.; Xu, W.; Zou, G.; Luo, H. *Nanoscale* **2016**, *8* (16), 8443–8465.
(15) Onozato, T.; Katase, T.; Yamamoto, A.; Katayama, S.; Matsushima, K.; Itagaki, N.; Yoshida, H.; Ohta, H. *J. Phys. Condens. Matter* **2016**, *28* (25), 255001.
(16) Fan, H.; Kim, H.-E. *J. Appl. Phys.* **2002**, *91* (1), 317–322.
(17) Yao, D. D.; Rani, R. A.; O'Mullane, A. P.; Kalantar-zadeh, K.; Ou, J. Z. *J. Phys. Chem. C* **2013**, *118* (1), 476–481.
(18) Tiano, A. L.; Koenigsmann, C.; Santulli, A. C.; Wong, S. S. *Chem. Commun.* **2010**, *46* (43), 8093–8130.
(19) Aegerter, M. A. *Sol. Energy Mater. Sol. Cells* **2001**, *68* (3), 401–422.
(20) Liu, M.; Xue, D.; Li, K. *J. Alloys Compd.* **2008**, *449* (1), 28–31.
(21) Shang, H.; Cao, G. In *Springer Handbook of Nanotechnology*; Springer, **2007**; pp 161–178.
(22) Fiz, R.; Hernandez-Ramirez, F.; Fischer, T.; Lopez-Conesa, L.; Estrade, S.; Peiro, F.; Mathur, S. *J. Phys. Chem. C* **2013**, *117* (19), 10086–10094.
(23) Merchan-Merchan, W.; Farahani, M. F. *Mater. Chem. Phys.* **2013**, *140* (2), 516–521.
(24) Fiz, R.; Appel, L.; Gutiérrez Pardo, A.; Ramírez-Rico, J.; Mathur, S. *ACS Appl. Mater. Interfaces* **2016** , 8 (33), 21423–21430.
(25) Li, L.; Deng, J.; Chen, J.; Sun, X.; Yu, R.; Liu, G.; Xing, X. *Chem. Mater.* **2009**, *21* (7), 1207–1213.
(26) Xu, C.-Y.; Zhen, L.; Yang, R.; Wang, Z. L. *J. Am. Chem. Soc.* **2007**, *129* (50), 15444–15445.
(27) Li, L.; Deng, J.; Chen, J.; Xing, X. *Chem. Sci.* **2016**, *7* (2), 855–865.
(28) Le Viet, A.; Jose, R.; Reddy, M. V; Chowdari, B. V. R.; Ramakrishna, S. *J. Phys. Chem.*

C **2010**, *114* (49), 21795–21800.
(29) Leindecker, G. C.; Alves, A. K.; Bergmann, C. P. *Ceram. Int.* **2014**, *40* (10), 16195–16200.
(30) Einarsrud, M.-A.; Grande, T. *Chem. Soc. Rev.* **2014**, *43* (7), 2187–2199.
(31) Mao, Y.; Park, T.-J.; Zhang, F.; Zhou, H.; Wong, S. S. *Small* **2007**, *3* (7), 1122–1139.
(32) Sochalski-Kolbus, L. M.; Wang, H.-W.; Rondinone, A. J.; Anovitz, L. M.; Wesolowski, D. J.; Whitfield, P. S. *Cryst. Growth Des.* **2015**, *15* (11), 5327–5331.
(33) Zhang, Z.; Zhang, G.; He, L.; Sun, L.; Jiang, X.; Yun, Z. *CrystEngComm* **2014**, *16* (17), 3478–3482.
(34) Luo, H.; Wei, M.; Wei, K. *J. Nanomater.* **2009**, *2009*, 35.
(35) He, J.; Hu, Y.; Wang, Z.; Lu, W.; Yang, S.; Wu, G.; Wang, Y.; Wang, S.; Gu, H.; Wang, J. *J. Mater. Chem. C* **2014**, *2* (38), 8185–8190.
(36) Wood, B. D.; Gates, B. D. In *MRS Proceedings*; Cambridge Univ Press, **2008**; Vol. 1087, 1087–1095.
(37) Uekawa, N.; Kudo, T.; Mori, F.; Wu, Y. J.; Kakegawa, K. *J. Colloid Interface Sci.* **2003**, *264* (2), 378–384.
(38) Zell, F. *Google Patents*, **2003**, 6,548,685.
(39) Bansal, N. P. *J. Mater. Sci.* **1994**, *29* (17), 4481–4486.
(40) Dalmaschio, C. J.; Ribeiro, C.; Leite, E. R. *Nanoscale* **2010**, *2* (11), 2336–2345.
(41) Zhu, G.; Zhang, S.; Xu, Z.; Ma, J.; Shen, X. *J. Am. Chem. Soc.* **2011**, *133* (39), 15605–15612.
(42) Hapiuk, D.; Masenelli, B.; Masenelli-Varlot, K.; Tainoff, D.; Boisron, O.; Albin, C.; Mélinon, P. *J. Phys. Chem. C* **2013**, *117* (19), 10220–10227.
(43) Wang, T.; Radovanovic, P. V. *J. Phys. Chem. C* **2010**, *115* (2), 406–413.
(44) Chhatre, A.; Duttagupta, S.; Thaokar, R.; Mehra, A. *Langmuir* **2015**, *31* (38), 10524–10531.
(45) Sajanlal, P. R.; Sreeprasad, T. S.; Samal, A. K.; Pradeep, T. *Nano Rev. Exp.* **2011**, *2*.
(46) Eastoe, J.; Tabor, R. *Surfactants and Nanoscience* **2014**, 135–157.
(47) Bakshi, M. S. *Cryst. Growth Des.* **2015**, *16* (2), 1104–1133.
(48) Qi, X.; Balankura, T.; Zhou, Y.; Fichthorn, K. A. *Nano Lett.* **2015**, *15* (11), 7711–7717.
(49) Zhang, Q.; Liu, S.-J.; Yu, S.-H. *J. Mater. Chem.* **2009**, *19* (2), 191–207.
(50) Wang, X.; Li, Z.; Shi, J.; Yu, Y. *Chem. Rev.* **2014**, *114* (19), 9346–9384.
(51) Mourdikoudis, S.; Liz-Marzán, L. M. *Chem. Mater.* **2013**, *25* (9), 1465–1476.
(52) Kim, Y.-K.; Min, D.-H. *Langmuir* **2012**, *28* (9), 4453–4458.
(53) Cheng, W.; Dong, S.; Wang, E. *Langmuir* **2003**, *19* (22), 9434–9439.
(54) Ozoemena, K.; Chen, S. *Nanomaterials for Fuel Cell Catalysis*; Springer, **2016**, 31–92.
(55) Yuan, Q.; Huang, D.-B.; Wang, H.-H.; Zhou, Z.-Y.; Wang, Q. *CrystEngComm* **2014**, 16 (13), 2560–2564.
(56) Koczkur, K. M.; Mourdikoudis, S.; Polavarapu, L.; Skrabalak, S. E. *Dalt. Trans.* **2015**, *44* (41), 17883–17905.
(57) Nguyen, T.-D. *Nanoscale* **2013**, *5* (20), 9455–9482.
(58) Li, A.; Xu, D.; Lin, H.; Yang, S.; Shao, Y.; Zhang, Y. *Sci. Rep.* **2016**, *6*.
(59) Liu, Y.; Tourbin, M.; Lachaize, S.; Guiraud, P. *Chemosphere* **2013**, *92* (6), 681–687.
(60) Grzelczak, M.; Sánchez-Iglesias, A.; Mezerji, H. H.; Bals, S.; Pérez-Juste, J.; Liz-Marzán, L. M. *Nano Lett.* **2012**, *12* (8), 4380–4384.
(61) Sperling, R. A.; Parak, W. J. *Philos. Trans. R. Soc. London A Math. Phys. Eng. Sci.* **2010**,

368 (1915), 1333–1383.
(62) Xu, L.; Ji, X.; Li, S.; Zhou, Z.; Du, X.; Sun, J.; Deng, F.; Che, S.; Wu, P. *Chem. Mater.* **2016**, *28* (12), 4512–4521.
(63) Maleki, M.; Beitollahi, A.; Shokouhimehr, M. *Eur. J. Inorg. Chem.* **2015**, *2015* (14), 2478–2485.
(64) Fan, W.; Zhang, Q.; Deng, W.; Wang, Y. *Chem. Mater.* **2013**, *25* (16), 3277–3287.
(65) Borchert, H.; Shevchenko, E. V; Robert, A.; Mekis, I.; Kornowski, A.; Grübel, G.; Weller, H. *Langmuir* **2005**, *21* (5), 1931–1936.
(66) Wang, Y.; Chan, S. L. I.; Amal, R.; Shen, Y. R.; Kiatkittipong, K. *Powder Diffr.* **2010**, 25, 217–217.
(67) Ungár, T. *Adv. Eng. Mater.* **2003**, *5* (5), 323–329.
(68) Rosen, M. J.; Kunjappu, J. T. *Surfactants Interfacial Phenomena, Fourth Ed.*; John Wiley & Sons, **2012**; 502–530.
(69) Morsy, S. M. I. *Int. J. Curr. Microbiol. App. Sci* **2014**, *3* (5), 237–260.
(70) Laurent, S.; Forge, D.; Port, M.; Roch, A.; Robic, C.; Vander Elst, L.; Muller, R. N. *Chem. Rev.* **2008**, *108* (6), 2064–2110.
(71) Bronstein, L. M.; Huang, X.; Retrum, J.; Schmucker, A.; Pink, M.; Stein, B. D.; Dragnea, B. *Chem. Mater.* **2007**, *19* (15), 3624–3632.
(72) Wang, Y.; Yang, H. *Chem. Commun.* **2006**, No. 24, 2545–2547.
(73) Zhao, Y.; Eley, C.; Hu, J.; Foord, J. S.; Ye, L.; He, H.; Tsang, S. C. E. *Angew. Chemie Int. Ed.* **2012**, *51* (16), 3846–3849.
(74) Backes, S.; Witt, M. U.; Roeben, E.; Kuhrts, L.; Aleed, S.; Schmidt, A. M.; von Klitzing, R. *J. Phys. Chem. B* **2015**, *119* (36), 12129–12137.
(75) Kang, Y.; Taton, T. A. *Angew. Chemie Int. Ed.* **2005**, *117* (3), 413–416.
(76) Thanh, N. T. K.; Green, L. A. W. *Nano Today* **2010**, *5* (3), 213–230.
(77) Wulandari, P.; Nagahiro, T.; Fukada, N.; Kimura, Y.; Niwano, M.; Tamada, K. *J. Colloid Interface Sci.* **2015**, *438*, 244–248.
(78) Vadivel, M.; Babu, R. R.; Arivanandhan, M.; Ramamurthi, K.; Hayakawa, Y. *RSC Adv.* **2015**, *5* (34), 27060–27068.
(79) Chen, J.; Lin, Y.; Jia, L. *J. Chromatogr. A* **2015**, *1388*, 43–51.
(80) Varade, D.; Haraguchi, K. *Soft Matter* **2012**, *8* (14), 3743–3746.
(81) Yang, Z.; Altantzis, T.; Zanaga, D.; Bals, S.; Tendeloo, G. Van; Pileni, M.-P. *J. Am. Chem. Soc.* **2016**, *138* (10), 3493–3500.
(82) Markvoort, A. J.; Pfleger, N.; Staffhorst, R.; Hilbers, P. A. J.; Van Santen, R. A.; Killian, J. A.; De Kruijff, B. *Biophys. J.* **2010**, *99* (5), 1520–1528.
(83) Tjipangandjara, K. F.; Somasundaran, P. *Adv. Powder Technol.* **1992**, *3* (2), 119–127.
(84) Bastús, N. G.; Comenge, J.; Puntes, V. *Langmuir* **2011**, *27* (17), 11098–11105.
(85) Song, S.-H.; Koelsch, P.; Weidner, T.; Wagner, M. S.; Castner, D. G. *Langmuir* **2013**, *29* (41), 12710–12719.
(86) Rubingh, D. *Cationic Surfactants: Physical Chemistry*; CRC Press, **1990**; Vol. 37, 87–140.
(87) Murayama, T.; Chen, J.; Hirata, J.; Matsumoto, K.; Ueda, W. *Catal. Sci. Technol.* **2014**, *4* (12), 4250–4257.

Supporting Information. The Supporting Information is available free of charge on the ACS Publications website at DOI: XXX . Figures S1 and S2 provide additional TEM images of control experiments, and Figure S3 includes the associated XRD data from these control experiments. Figure S4 includes the electron diffraction analysis of the Nb_2O_5 nanorods. Figures S5 and S6 present Raman spectroscopy results from the nanorods prepared both with and without the addition of surfactants, and Figures S7 through S9 present additional data (TEM, XRD and size distributions) for the systematic investigation into varying the concentration of SDS added to the reaction mixture. Additional information is presented on the critical micelle concentrations reported in the literature for some of the surfactants used in these studies (Table S1), and dynamic light scattering analysis of suspensions with varying concentrations of SDS (Figure S10).

For Table of Contents Use Only

Surfactant Controlled Growth of Niobium Oxide Nanorods

Rana Faryad Ali,[†,‡] Amir H. Nazemi,[†,‡] Byron D. Gates[*,†]*

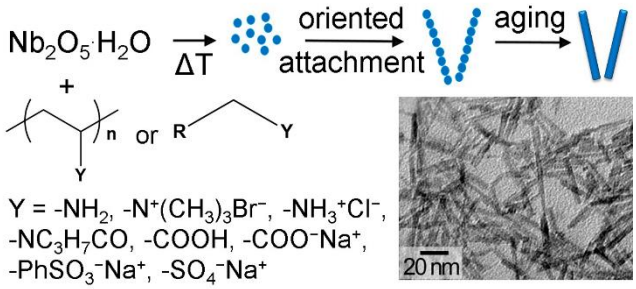

This study demonstrates a solution-phase synthesis of uniform single-crystalline nanorods of niobium oxide (Nb_2O_5) using a process of oriented attachment. The reaction mixture was systematically studied through the addition of surfactants, which provided insight into controlling crystal formation and growth. Regularity of the dimensions and shapes of the product can be tuned by adjusting the composition and concentration of these surfactants.